Geomechanical model for fracture deformation under hydraulic, mechanical and thermal loads

Chris McDermott · Olaf Kolditz

Abstract Hydraulic flow and transport (heat and solute) within crystalline rocks is dominated by the fracture systems found within them. In situ stress conditions have a significant impact on the hydraulic, mechanical and thermal coupled processes, and quantification of these processes provides a key to understanding the often transient time-dependent behaviour of crystalline rocks. In this paper, a geomechanical model is presented which describes fracture closure as a function of effective stress and the changes in parameters such as storage, permeability, porosity and aperture. Allowing the fracture closure to be defined by the change in normal effective stress provides a link to the numerical consideration of parametrical changes due to rock stress alterations caused for example by changes in fracture fluid pressure, stress release, tectonic stress, thermal stress, orientation of the natural fracture in the pervasive stress system and local changes in a rock mass due to stress alteration. The model uses geometrical considerations based on a fractal distribution of apertures on the fracture surface, and applies well-established analytical elastic deformation solutions to calculate the deformation response to changes in effective stress. Analysis of the fractal generation method allows a standard normal distribution of fracture apertures to be predicted for all common fractal dimensions relating to a 2D surface. Changes in the fracture aperture are related to hydraulic functions such as permeability, storage and porosity of the fracture. The geomechanical model is experimentally validated against laboratory scale experimental data gained from the closure of a fractured sample recovered at a depth of 3,800 m from the KTB pilot borehole. Parameters for matching the experimental data were established externally, the only fitting parameters applied were the minimum and maximum contact area between the surfaces and the number of allowable contacts. The model provides an insight into the key processes determining the closure of a fracture, and can act as a material input function for numerical models linking the effects of changes in the stress field, hydraulic or thermal conditions, to the flow and transport parameters of a fractured system.

Résumé L'écoulement et le transport (chaleur et soluté) dans les roches cristallines sont dominés par les systèmes de fracture. Les conditions de stress in-situ ont un impact significatif sur l'hydraulique, les processus couplés de mécanique et thermique et la quantification de ces processus apportent une clé pour comprendre le comportement transitoire des roches cristallines. Dans cet article un modèle géomécanique est présenté, modèle qui décrit la fermeture des fractures comme une fonction de la contrainte effective et des changements de paramètres tels le coefficient d'emmagasinement, la perméabilité, la porosité et l'ouverture. En s'accordant que la fermeture des fractures est définit par les changements de la contrainte effective normale, on apporte le lien avec la considération numérique des changements paramétriques dus aux altérations de la contrainte des roches, causés par exemple par des variations de la pression des fluides dans les fractures, du dégagement de la contrainte, des contraintes tectoniques et thermiques, des orientations des fractures naturelles dans le système de contraintes pénétrantes, et des changements locaux dans un massif de roches dus à l'altération des contraintes. Le modèle utilise des considérations géométriques basées sur une distribution fractale des ouvertures à la surface des fractures, et permet d'établir des solutions analytiques de la déformation élastique pour calculer la réponse de la déformation à la contrainte effective. L'analyse de la méthode par génération fractale permet de prédire une distribution normale standard de l'ouverture des fractures, pour toutes les dimensions fractales en relation avec les surfaces 2D. Les changements dans l'ouverture des fractures sont mis en relation avec les fonctions hydrauliques tels la perméabilité, l'emmagasinement et la porosité de la fracture. Le modèle géoméchanique est expérimentalement validé à l'échelle du laboratoire sur un échantillon fracturé récupéré à une profondeur de 3,800 mètres sur le puits du site pilote KTB. Les paramètres du calibrage des données expérimentales ont été établies extérieurement, les seuls paramètres utilisés étant les surfaces de contact minimum et maximum, et le nombre de contacts permis. Le modèle apporte une connaissance perspicace sur le processus clé

Received: 16 February 2005 / Accepted: 1 March 2005
Published online: 8 September 2005

C. McDermott (✉) · O. Kolditz
Center for Applied Geoscience, Chair of GeoSystems Research,
University of Tübingen,
72076 Tübingen, Germany
e-mail: chris.mcdermott@uni-tuebingen.de

 DOI 10.1007/s10040-005-0455-4

déterminant la fermeture des fractures, et peut servir de fonction input dans les modèles numériques reliant les effets des variations de la contrainte du terrain, les conditions hydrauliques ou thermales, les paramètres de l'écoulement et du transport et les systèmes de fracture.

Resumen El flujo hidráulico y transporte (de calor y solutos) dentro de rocas cristalinas está dominado por los sistemas de fracturas que se encuentran en ellas. Las condiciones de esfuerzos in-situ tienen un impacto significativo en los procesos aparejados termales, mecánicos e hidráulicos y la cuantificación de estos procesos aporta una clave para entender el frecuente comportamiento transitorio dependiente de las rocas cristalinas. En este artículo se presenta un modelo geomecánico que describe el cierre de fracturas en función del esfuerzo efectivo y los cambios en parámetros tal como almacenamiento, permeabilidad, porosidad y apertura. El definir el cierre de fractura mediante el cambio en esfuerzo normal efectivo aporta un vínculo con la consideración numérica de cambios paramétricos ocasionados por alteraciones de esfuerzos en la roca causadas, por ejemplo, por cambios en presión de fluidos en fractura, liberación de esfuerzo, esfuerzo tectónico, esfuerzo termal, orientación de fracturas naturales en el sistema de esfuerzos penetrante, y cambios locales en una masa rocosa ocasionados por alteración de esfuerzos. El modelo utiliza consideraciones geométricas basadas en la distribución fractal de aperturas en la superficie de fractura y aplica soluciones analíticas bien establecidas de deformación elástica para calcular la respuesta de deformación a cambios en el esfuerzo efectivo. Los análisis del método de generación fractal permiten predecir una distribución normal standard para la distribución de aperturas de fracturas para todas las dimensiones fractales comunes que se relacionan con una superficie 2D. Los cambios en la apertura de fractura se relacionan con funciones hidráulicas tal como permeabilidad, almacenamiento y porosidad de la fractura. El modelo geomecánico se ha validado experimentalmente en contra de datos experimentales a escala de laboratorio obtenidos a partir del cierre de una muestra fracturada recuperada a una profundidad de 3,800 m en el pozo piloto KTB. Se establecieron externamente parámetros que se ajustan a los datos experimentales, con los parámetros de ajuste aplicados que fueron el área máxima y mínima de contacto entre las superficies y el número de contactos permisibles. El modelo arroja luz sobre los procesos clave que determinan el cierre de una fractura y puede actuar como un material de función de entrada para modelos numéricos que vinculan los efectos de cambios en el campo de esfuerzos, condiciones termales o hidráulicas, con los parámetros de flujo y transporte de un sistema fracturado.

Introduction

Application

Understanding the hydraulic flow and transport (heat and solute) within crystalline rocks is particularly important in fields such as the utilisation of crystalline hot dry rock geothermal reservoir systems at depths of at least 4 km, (e.g. Baria et al. 1999; O'Sullivan et al. 2001), or prediction of the behaviour of radioactive nuclide migration (e.g. National Coorperative for the Disposal of Radioactive Waste (NAGRA), Buscheck et al. 2002). The transport characteristics of crystalline rocks are dominated by the fracture systems found within them. In situ stress conditions have a significant impact on the parameters of the fracture system responsible for flow and transport (e.g. Rutqvist and Stephanson 2003; Kessels 2000), and quantification of the hydraulic, thermal and mechanical coupled processes provides a key to understanding the behaviour of crystalline rocks.

Fracture systems dominate the mass and energy transport of deep crystalline rocks (e.g. Emmermann and Lauterjung 1997). The characteristics of the three dimensional fracture systems in terms of flow, transport and heat conduction are controlled by a number of critical factors, in particular the geometry of the system in terms of the orientation of the fractures in the pervasive stress system (e.g. Zimmermann et al. 2000, 2003), the fracture connectivity (e.g. Bour and Davy 1997; Manzocchi 2002), fracture permeability (e.g. Nicholl et al. 1999; Wang et al. 1988; Watanabe and Takahashi 1995), porosity (e.g. Montemagno and Pyrak-Nolte 1995) and area of fracture system available for sorption and heat exchange (e.g. Renner and Sauter 1997; Wels et al. 1996) form some of the most important factors which need to be addressed.

One important aspect highlighted by a number of authors regarding the long-term behaviour of fracture systems is their response to stress changes which may be generated due to hydraulic alterations of the systems, long-term stress field alterations (erosion considerations during waste deposition storage), and thermo-elastic stress alterations due to a change in the amount of heat in the systems (hot dry rock heat extraction). Indeed O'Sullivan et al. (2001) particularly pointed out that long-term geo-mechanical effects of thermal stress changes on geothermal reservoir characteristics need to be investigated. A model is presented here where effective stress across a fracture is linked to the fracture aperture, permeability and effective porosity. The effective stress is a function of the tectonic stresses, the hydraulic stresses and thermal stress release (McDermott et al. 2005).

In situ conditions at depth

For deep-seated fracture systems, pressure heads of the order of several hundred meters can be expected, particularly in the case of injection or extraction of fluids for the recovery of geothermal energy. This therefore greatly increases the pressure-dependent effects in fracture systems, usually not seen in near surface hydrogeological considerations where comparatively small head changes are encountered. Additionally during HDR operation, as a consequence of heat energy extraction temperature differences of the order of 100°C can be expected, which in turn leads to large amounts of stress energy release.

 DOI 10.1007/s10040-005-0455-4

The response of a fracture network to stimulation by either extraction or injection of fluid and temperature changes is a time-dependent integral signal comprising the individual responses of the discrete fractures (e.g. McDermott et al. 2003; Beeler and Hickman 2004). The individual responses of the discrete fractures within the fracture system are determined by interaction of the fluid injected or extracted and its physical characteristics such as density, viscosity, heat capacity and temperature. Within the solid medium factors such as the elastic response of the medium and pervasive in situ conditions including temperature and pressure have a critical impact. Alterations within the fracture system of parameters such as the contact area, storage, effective porosity, flow channelling and permeability can be expected coupled to changes in the pervasive conditions.

Existing models

Both empirical solutions and elastic models are currently applied to investigate fracture opening and closure in response to stress alterations. Rutqvist and Stephanson (2003) provides an excellent overview of models used for hydromechanical coupling at an aquifer level, and a number of well-known empirical approaches to changes in the normal stress across fractured medium. Zimmerman (1991) published an important monograph on the compressibility of sandstones, including much work on stress and the deformation of different shapes of pore spaces as well as including a number of analytical solutions for deformation. Papanastasiou (2000) and Bai et al. (2000) applied elastic solutions for rock masses after Jaeger and Cook (1979) for elliptical cracks to define the deformation responses of fractures under tectonic extension in multiple layered systems. This approach views the fracture as an ellipse, which can open or shut, but ignores the impact of asperities in the fractures. Myer (2000) developed a similar model, where the fracture is represented by several coplanar ellipses simulating cracks. The closure of the fracture is related to the contact area between the ellipse where the fracture is assumed to be closed, the interaction of the ellipses with each other, and the elastic solutions for the collapse of an ellipse in a given stress field. On the other hand, Greenwood and Williamson (1966) proposed a model defining the fracture asperity height with a probability density function. This model coupled with a Hertzian deformation, Johnson (2001), of the asperity tips and the detailed consideration of contact stress of asperities linked with the resulting contact area of the asperities is often used as a starting point for the prediction of fracture aperture closure or expansion dependent on normal stress, (e.g. Brown and Scholz 1985). Beeler and Hickman (2001) presented a non Hertzian model for the closure of a rough fracture where not just the tip area of asperity contact is considered but the entire contacting height of the asperities are taken into account, however the effect on the rock mass was not included.

Overview of the geomechanical model premises and application

In this paper, an elastic model for the closure/opening of a fracture under changes in effective stress is presented. Here the far field stress conditions, the asperity distribution and the development of contact between the fracture surfaces is considered. A key assumption to this model is that the aperture distribution can be represented as a fractal function, (e.g. Ogilvie et al. 2003; Fomin et al. 2003; Babadagli and Develi 2000; Glover et al. 1999; Watanabe and Takahashi 1995; Belfield 1994; Wang et al. 1988). The use of a fractal distribution provides a number of advantages, in particular the system can be considered either as a two dimensional closure and contact of a number of asperities (i.e. aperture and length are considered), or three dimensional closure of two fracture planes (aperture length and depth). The mathematics and distribution of the asperities are principally identical in each case due to the inherent self-similarity of the fractal distributions, apart from the addition of a second dimension when moving from a line to a surface generation, (Zhou and Xie 2003). This important property coupled with averaging techniques and the application of a number of established soil and rock mechanic formulas for settlement in elastic half space under loading originating from the famous Boussinesq approach for point loads (Boussinesq 1878), and the application of spatial integration of this theory to define several shape-dependent analytical solutions (e.g. Poulos and Davis 1974; Davies and Selvadurai 1996) allows the simplified consideration of what is a complex system under closure. All the closure modelling and prediction of the hydraulic parameters of the fracture presented here were undertaken using Excel worksheets.

The fracture response is considered to be totally elastic and the possible time dependency of closure is assumed to be negligible given the relatively short period of time over which the amount of closure alters in comparison to the length of time of the processes being investigated. Time-dependent closure has been recently investigated by Matsuki et al. (2001), who considered time-dependent closure of fractures under the normal stress as determined by Brown and Scholz (1985) for fractures comprising a given probability function distribution of aperture sizes. Their results indicated that within 40 h the system had reached stable conditions, and that most of the response of the fractures to external stress changes happened within a matter of hours of application. The model developed here is used to define and model long-term changes in the fracture systems, i.e. longer than 40 h. Very long-term effects such as viscous closure are not included at this stage.

A big advantage of this geomechanical fracture closure model is that it considers changes in effective stress in the fracture plane and allows an increase in contact area of the fracture surface. This allows consideration of both external loading, changes in the porewater pressure (e.g. fluid injection or extraction) or changes in thermal stress. The change in contact stress resulting from the change in effective stress

 DOI 10.1007/s10040-005-0455-4

is considered to be uniformly distributed throughout the asperities, and therefore the cumulative contact stress at each point is not important, rather the change in the stress and the associated deformation. The effects of possible mechanical damage, hysterisis and shear movement are not included.

The whole rock body is considered to be involved in the deformation and not just the asperities themselves, although naturally they are predominant factors in deformation of the fracture. Taking this into account reduces the problem of unrealistically high contact strains as commented upon by Beeler and Hickman (2001) and predicted by some Hertzian based models.

The elastic response is defined by the elastic constants Poisson's ratio (u) and the elastic modulus (E) in Pa, there is no need for a time-dependent relaxation modulus. As the model approaches the evaluation of the increase in stress stepwise, so changes in the elastic constants due to changes in pressure and temperature can be taken into account.

The model has been applied to match the experimental closure of a fracture taken from a sample of rock from a depth of 3,800 m in the KTB pilot hole, Durham (1997). The key parameters for the model were field and laboratory measured elastic parameters, an estimation of the starting contact area as a percentage of the fracture profile, and the starting number of contacts between the fracture surfaces and the maximum number of contacts possible between the fracture surfaces.

The model

Model concept

Conceptually, the fracture plane is considered to comprise two non-perfectly matching surfaces, where the heights of the asperities on the surfaces are described by a fractal distribution (e.g. Glover et al. 1999; Xie et al. 1999; Zhou and Xie 2003; Ogilvie et al. 2003). The fracture surface is considered only in the planar i.e. aperture and length, and not depth. This assumption is valid in terms of understanding the compressive response of the fracture as the fractal distribution in two or three dimensions will be constant.

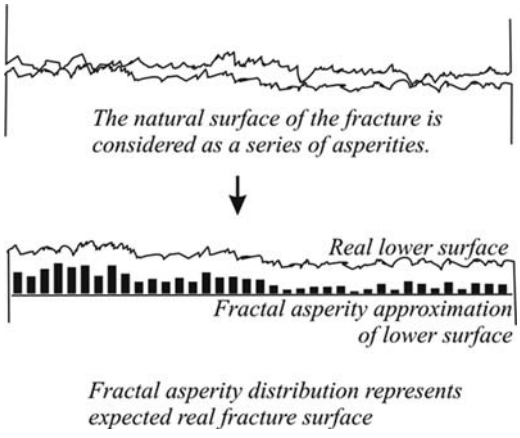

Fig. 1 The fracture is represented as a series of asperities of different heights, the heights of the asperities follows a fractal distribution

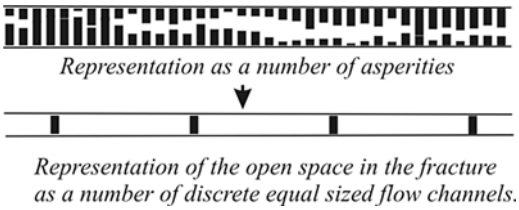

Fig. 2 The asperity distribution is converted to a fracture comprising equal volume channels and a certain number of contacts. The total volume of the fracture remains constant

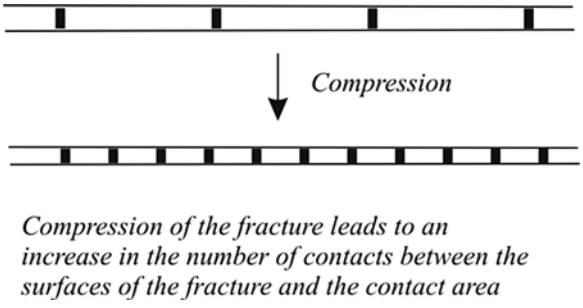

Fig. 3 Increase in the number of contacts in the fracture as compression reduces the size of the aperture

This assumption, is, however, not carried through to the calculation of permeability as this would then be a function of the harmonic mean (e.g. Baraka-Lokmane et al. 2003); for permeability the third dimension is considered.

The fracture is conceptually presented as a series of asperities (Fig. 1) which on closure form a number of flow channels of equal width. The number of contacts between the upper and lower surface of the fracture is given by the fractal distributed asperity heights. The volume of the fracture represented by the asperity distribution and that represented by the flow channels of equal width is equal, (Fig. 2). Further compression of the fracture increases the number of contacts between the two surfaces and therefore the number of flow channels (Fig. 3).

Detailed realisation of fracture closure model

To aid the understanding of the methodology behind this geomechanical model, the model is illustrated by sequentially following the steps involved in calculation of the closure under a stress increment. The rock mechanical parameters poisons ratio (υ) and the elastic modulus (E), as well as the density and compressibility of the fluid in the fractures can be coupled to the pressure and temperature conditions. The initial volume of the fracture prior to any stress change is given, as is the ratio of contact area to non-contact area of the fracture surfaces, the starting number of contacts, and the maximum number of contacts. Incrementally with stress increase steps (1)–(6) below are repeated in Fig. 4. Here a short overview of the steps is given, a detailed description of the steps and the assumptions is given in the following sections.

Step (1): Fracture geometry. The fractal geometry of the fracture is calculated including the number of contacts

 DOI 10.1007/s10040-005-0455-4

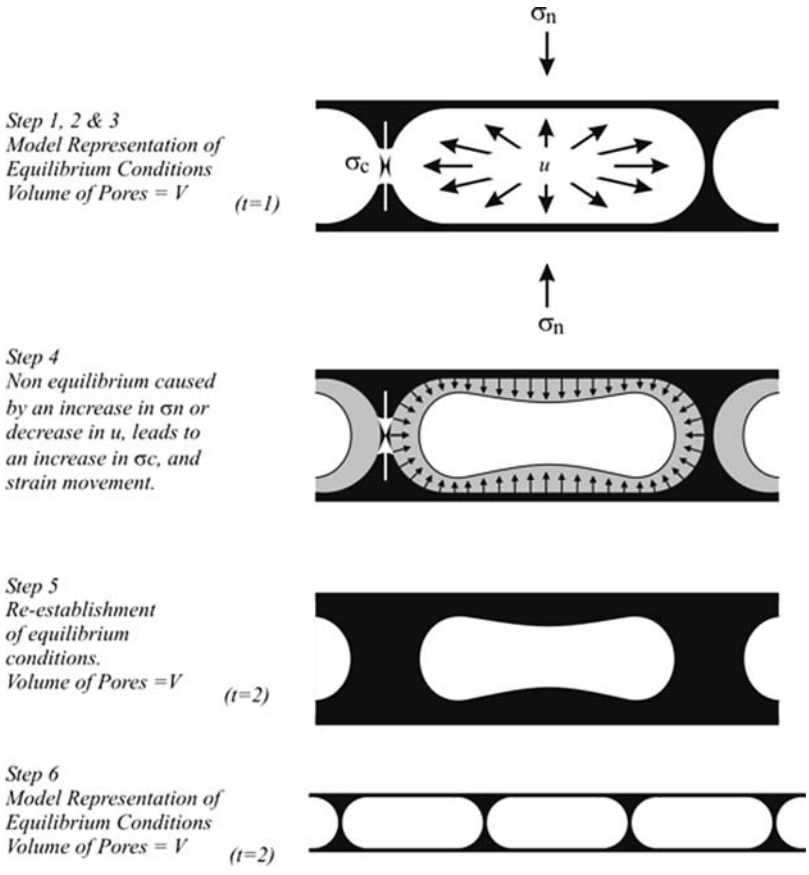

Fig. 4 Modelling of incremental closure of the fracture

between the upper and lower surface and the volume of the open space between the fracture surfaces.

Step (2): Channel geometry. The dimensions of the individual channels between the contacts between the upper and lower surfaces, the volume of contacts and areas of the contacts are calculated.

Step (3): Stress conditions. The model increases or decreases stress stepwise. Here the stepwise change of stress is broken down into the change of stress within the various geometrical elements.

Step (4): Fracture deformation. The deformation of the various geometrical elements is calculated

Step (5): Next time step fracture geometry. The new fracture volume is calculated based on the sum of the deformation.

Step (6): Fracture parameters. The parameters in terms of porosity, aperture, permeability and storage release are determined based on the change of volume and the new fracture volume are calculated.

Fracture geometry

Generating a fracture surface applying a fractal approach, (e.g. Zhou and Xie 2003; Glover et al. 1998a, 1998b) leads to good representation of a typical rock surface. In particular, the asperity distribution can be shown to be Gaussian normally distributed (e.g. Glover et al. 1998b). Zhou and Xie (2003) shows that using a random Brownian function (B) the probability (P) distribution of an increment on the surface is given by

$$P\left(B\left(x+h, y+k\right)-B\left(x, y\right) \leq z\right) = \frac{1}{\sqrt{2\pi}\left(h^2+k^2\right)^{-\frac{H}{2}}} \times \int_{\infty}^{z} \exp\left(\frac{-r^2}{2\left(h^2+k^2\right)^{H}}\right) \mathrm{d}r \quad (1)$$

where x and y represent Cartesian coordinates on a fracture surface, h and k are the incremental differences, z is the mean asperity height, r is the distance $\sqrt{h^2+k^2}$ and H is the Hausdorff dimension (Hausdorff 1919). The fractal surface dimension is given by 3-H (Zhou and Xie 2003). By normalising both the number of contacts allowed between the upper and lower surface of a fracture, and the size of the aperture it can be seen that Eq. (1) reverts to a normal Gaussian probability density function.

$$P = \frac{1}{\sigma\sqrt{(2\pi)}} \exp\left(\frac{-(x-\mu)^2}{2\sigma^2}\right) \quad (2)$$

where μ is the mean, x is the variable, and ρ^2 in this case is the variance (Evans et al. 2000). Using the fractal surface generator SynFrac, available from Aberdeen University Petrophysics Group, Glover et al. (1999), the asperity distribution was determined, normalised and fitted using a polynomial fit (Fig. 5). The polynomial fit is given by

$$nc = mnc(0.994 + 0.224x - 2.256x^2 + 1.563x^3$$

 DOI 10.1007/s10040-005-0455-4

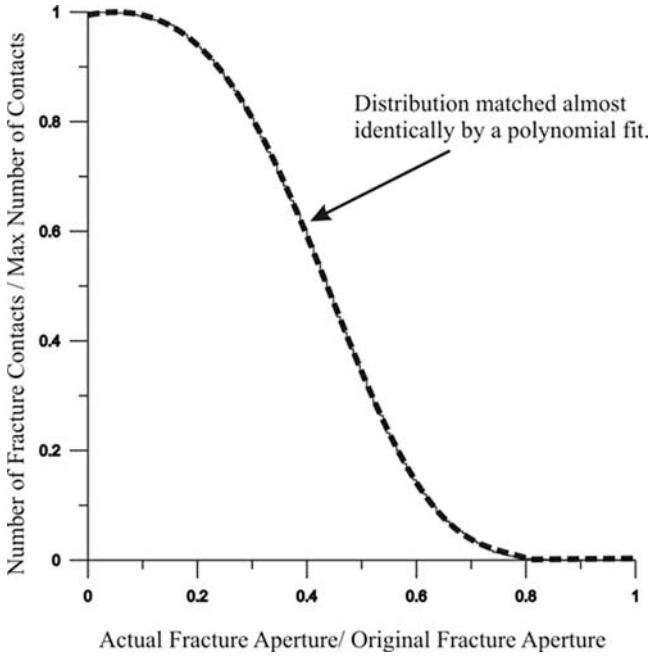

Fig. 5 Normalised distribution of the number of contacts between the fracture surfaces against the aperture closure of the fracture

$$-10.167x^4 - 50.550x^5 + 220.217x^6 \\ -254.595x^7 + 94.573x^8) + snc \quad (3)$$

where x represents the degree of closure of the fracture, 0 being totally closed, 1 being open, nc is the number of contacts, mnc is the maximum number of contacts possible and snc is the starting (minimum) number of contacts. The number of contacts between the surfaces of the fracture is the key element in determining the closure behaviour of the fracture. The statistical distribution of the contact heights, and thereby the number of contacts between the fracture surfaces under a certain load provides the key to understanding the form of the closure curve, and the parameters coupled to this behaviour.

The fracture volume f, (m^3) is considered to comprise both the open spaces of the fracture and the contacts Eq. (4)

$$f_v = ncC_{\text{av}} + ncC_{\text{hv}} \quad (4)$$

where $C_{>\text{av}}$ is the volume of a contact and C_{hv} is the volume of a channel. The initial volume of the fracture is set as an input parameter. After steps 1–6 are completed, the new changed volume of the fracture as a result of that increment of stress and associated deformation is calculated and used as an input parameter for the next increment of stress.

Channel geometry

The channel geometry (Fig. 6) is calculated from three parameters,

– The total volume of the fracture, f_v.
– The number of contacts forming channels nc.
– The total area of the existing contacts tCa.

$$tC_a = \frac{ncC_{av}}{f_a} \quad (5)$$

where f_a is the total unit area (m^2) of the fracture, taken as 1 m^2. Each of these three parameters is recalculated in every stress increment during the execution of steps 1–6. The geometry of the channels (Fig. 7) is determined from the volume of the fracture available to flow. The width of the channel, x(m), is approximated by

$$x = \frac{f_v tC_a}{ncf_a} \quad (6)$$

The value r represents half the aperture of the fracture openings, and is taken to represent the radius of the end sections of the fracture openings. The quadratic solution for r can be found from the following expression of the fracture volume for a unit width:

$$f_v = ((x - 2r)2r + \pi r^2)nc \quad (7)$$

The plausible value of r is applied to define the channel geometry, the aperture of the channel e(m) is given by.

$$e = 2r \quad (8)$$

Assuming a simple rectangular type contact, the contact area of each contact Ca can then be represented by Eq. (9)

$$\text{Ca} = \frac{ncC_{\text{av}}}{f_a 2r} \quad (9)$$

Stress conditions

The fluid pressure (u), the average contact stress (σ_c), and the normal stress (σ_n) need to be calculated at this stage, all given in Pa. The effective stress (σ') is given after Smith and Smith (1998) by:

$$\sigma' = \sigma_n - u \quad (10)$$

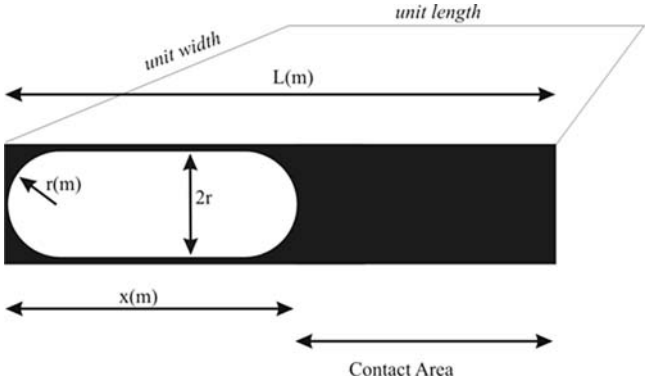

Fig. 6 Determination of channel geometry

DOI 10.1007/s10040-005-0455-4

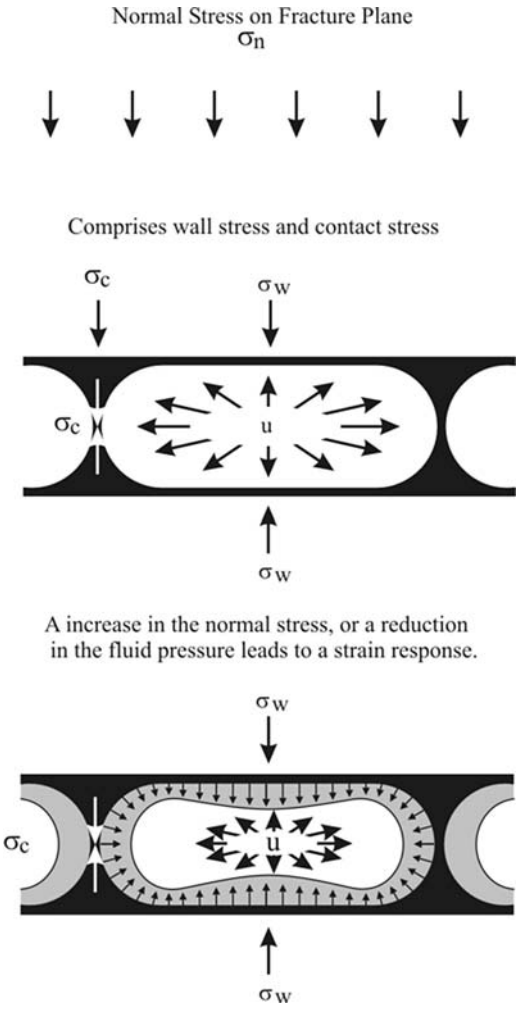

Fig. 7 Wall stress, contact stress, deformation

The normal stress on a fracture plane orientated with directional cosins l, m, n, to the stress axes $\sigma_x, \sigma_y, \sigma_z$ respectively and forming the normal vector $\hat{n}$ to the plane is given after Davies and Selvadurai (1996) as

$$\sigma_n = \left(\sigma^T \hat{n}\right) \cdot \hat{n} \tag{11}$$

where

$$\sigma = \begin{bmatrix} \sigma_x & \tau_{xy} & \tau_{xz} \\ \tau_{yx} & \sigma_y & \tau_{yz} \\ \tau_{zx} & \tau_{zy} & \sigma_z \end{bmatrix} \tag{12}$$

and

$$\hat{n} = \begin{bmatrix} l \\ m \\ n \end{bmatrix} \tag{13}$$

Here τ represents shear stress. The normal stress comprises what the authors term wall stress (σ_w) and contact stress (σ_c) (Fig. 8). The wall stress represents the difference between the surrounding normal stress and the fluid pressure

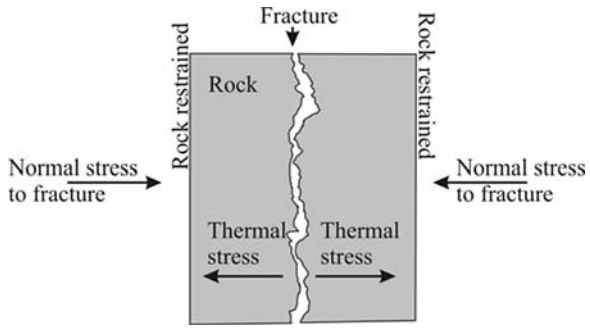

Fig. 8 Inclusion of thermal stress

in the fracture, the contact stress is the stress carried across the contacts in the fracture maintaining the fracture aperture. Here wall stress is used rather than the term effective, similarly defined, to show that the areas where asperities contact are not considered.

When the fluid pressure (u) is reduced, the normal stress does not change. The wall stress changes by the change in the fluid pressure, positive towards the fracture plane, and the contact stress increases by the effective stress increase divided by the area of the contacts Eq. (14). This derivation is proved for a 3D porous body by Zimmerman et al. (1994), and here applied for the model representation of the fracture plane.

If external confining pressure is applied, i.e. loading, the wall stress increases again positive towards the fracture plane by the difference to the fluid pressure and the contact stress increases by the effective stress increase divided by the area of the contacts.

$$\Delta\sigma_c = \frac{\Delta\sigma'}{tCa} \tag{14}$$

For fluid pressure alteration

$$\Delta\sigma_w = \Delta u \tag{15}$$

or for a change in normal stress

$$\Delta\sigma_w = \Delta\sigma_n \tag{16}$$

At this point it is possible to see that the change in effective stress can either be given by a decrease in the fluid pressure (u) or an increase in the normal stress (σ_n). This means by considering effective stress both the effects of fluid extraction or injection can be considered as in the case of a geothermal reservoir (e.g. McDermott et al. 2005), or an increase in confining pressure on the sample as in laboratory compression tests (e.g. Durham 1997).

Thermal stress arises as a result of the change in temperature in the rock system. In the case of the extraction of heat from a fractured rock, for example the Hot Dry Rock application (e.g. O'Sullivan et al. 2001), colder water is pressed through the fracture. Cooling of the block can then as a first approximation be assumed to be normal to the fracture

DOI 10.1007/s10040-005-0455-4

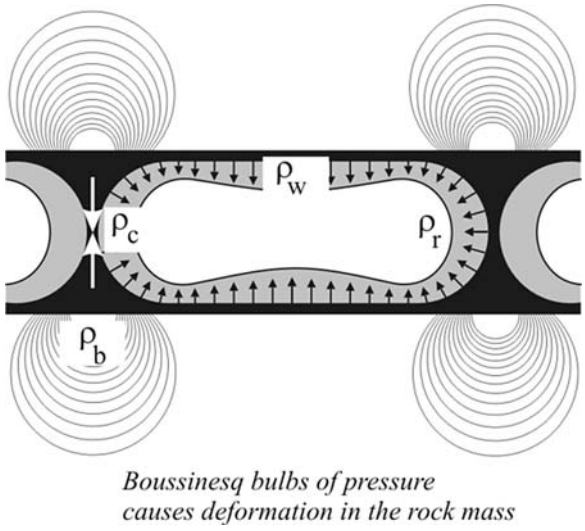

Fig. 9 Deformation resulting from an increase in effective stress in fracture model

plane, and therefore the thermal stresses be operating normal to the fracture plane. In more complicated geometries, such as the presence of several fractures in a shear zone, or a predominant thermal gradient, this assumption will break down and a more detailed analysis of the direction of the thermal stress may be required. Additionally, as cooling progresses in more complex systems the principal directions of the thermal stress will alter (work in progress). In the current model, the thermal stress caused by cooling is assumed to work normal to the fracture plane and in an opposite direction to the normal tectonic stress. The thermal stress, σ_t, can be approximated by Eq. (17) assuming no viscous flow in the rock.

$$\sigma_t = K_r E \alpha \Delta T \tag{17}$$

Here E is the modulus of elasticity, α is the thermal expansion coefficient, ΔT is the change in rock temperature and K_r is the coefficient of mechanical restraint. The value K_r, has a value of 1 in fully restrained systems where no movement is possible, and where movement is possible its value drops rapidly.

The effective stress across the fracture relating to Fig. 9 is given by

$$\sigma' = \sigma_h - (u + \sigma_t) \tag{18}$$

The mechanical restraint to thermal contraction and the development of the thermal stresses is dependent on the complex geometry of the rock fractures within the rock mass. Characterisation of the rock mass features is notoriously difficult (e.g. Barton and Bandis 1990; Bieniawski 1989; Laubscher 1977). Further research in the area of understanding mechanical restraint to thermal contraction in rock masses is required, (e.g. JNC 1999).

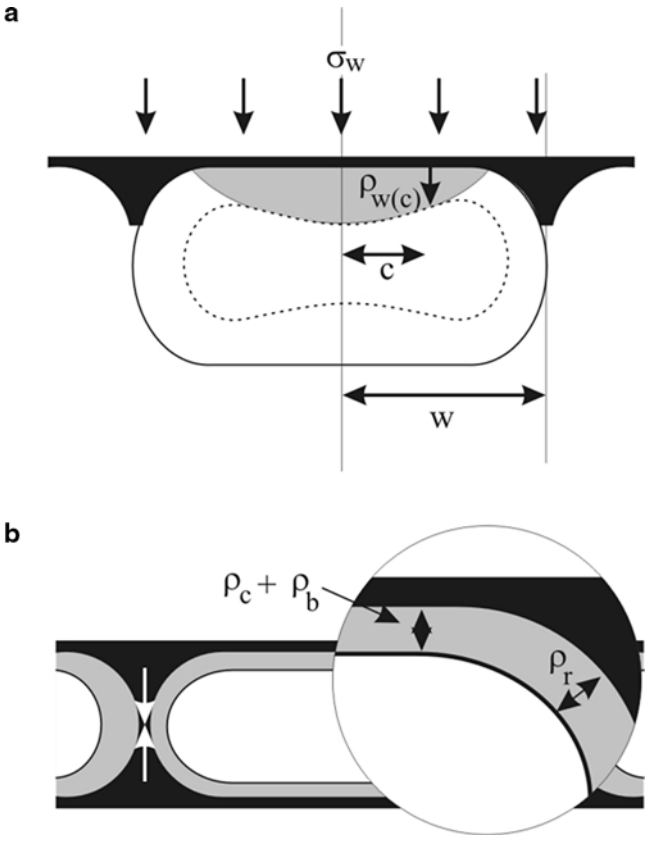

Fig. 10 Inward movement of the fracture wall as a consequence of a reduction in fluid pressure or increase in normal stress

Fracture deformation

The solid deformation due to the change in effective stress is modelled as a combination of four factors in the rock wall (Fig. 10):

1. Fracture wall deformation (ρ_w)
2. Fracture column deformation (ρ_c)
3. Fracture base deformation (ρ_b)
4. Fracture end deformation (ρ_r)
   Furthermore fluid deformation (ρ_f) in terms of pressure changes in the fluid can also be considered.
5. Fluid deformation (ρ_f)

Fracture wall deformation (ρ_w). To determine the fracture wall deformation (ρ_w) firstly the displacement of the fracture wall is calculated after Poulos and Davis (1974):

$$\rho_w = 2(1 - \upsilon^2)\frac{\Delta\sigma_w}{E}(c^2 - w^2)^{\frac{1}{2}} \tag{19}$$

Here σ_w is the wall stress, c and x are geometric terms described in Fig. 10a. The value of ρ_w is given at a distance c from the centre of the channel. This formulation is similar to that used by Bai et al. (2000) for the prediction of elliptical fracture aperture under tectonic stress and by Myer (2000).

Once the number of contacts has increased to the extent that the length of the fracture is similar to the aperture, the

 DOI 10.1007/s10040-005-0455-4

fracture is represented by a circle and the wall deformation is no longer significant. The circular representation is inherent in the consideration of the fracture end deformation given below.

Fracture column deformation (ρ_c). Column deformation, comprises a compression parallel to the contact stress (ρ_v) and a lateral expansion normal to the contact stress (ρ_l)

$$\rho_v = \frac{2r\,\Delta\sigma_c}{E} \tag{20}$$

$$\rho_l = \frac{Ca\upsilon\,\Delta\sigma_c}{E} \tag{21}$$

Fracture base deformation (ρ_b). The deformation of the base of the fracture is estimated by applying analytical solutions for the deformation of strip footings on elastic material as given by Giroud (1968) and summarised by Poulos and Davis (1974). Here the following formulation is derived for the specific case to derive the mean settlement

$$\rho_b = \frac{Ca\Delta\sigma_c\left(1-\upsilon^2\right)}{E} I \tag{22}$$

I is an influence factor depending on the geometry of the strip footing. For all the calculations the fracture was assumed to have a length of 1 m. Fitting data from Poulos and Davis (1974) this can be given as

$$\begin{aligned} I &= A\ln\left(\frac{1}{Ca}\right) + B \\ A &= 0.6235242847 \\ B &= 0.85039655706 \end{aligned} \tag{23}$$

Fracture end deformation (ρ_r). As the number of contacts increase so the formulation of the fracture end deformation becomes more important than the formulation of the fracture wall deformation. Again, analytical solutions are used from the field of elastic analysis, and a particularly interesting effect is observed. The end of the fracture area is considered to be equivalent to a circular opening in a uniform stress field. The change in stress is given by the change in the fluid (u) or wall pressure.

$$\rho_r = \frac{2\left(1-\upsilon^2\right)}{E}\Delta ur \tag{24}$$

derived from Poulos and Davis (1974)

It is interesting to note at this stage that in Eq. (24), the displacement is a function of the original radius of the hole. In the case of a large number of contacts, as would be expected under high effective stress loads, the formulation of the closure problem should reduce eventually to Eq. (24). With increasing closure pressure, the hole gets smaller, but never actually closes. It should be noted that this formula is valid for incremental displacements, and gives an incorrect answer if one extremely large stress increment is applied instantaneously.

Examining this formula and allowing only elastic deformation of rock materials in non-perfectly fitting fracture surfaces, it can be seen that it is impossible by normal stress alone to cause the fractures to be closed. There will always be a residual opening. Closure must therefore be due to a secondary influence such as deposition of minerals, plastic deformation, or shear and breaking movements.

Fluid deformation (ρ_f). Fluid deformation is given by

$$\rho_f = C_f\,\Delta u \tag{25}$$

where C_f is the fluid compressibility under the respective temperature and pressure conditions.

Fracture geometry after stress increment

The new fracture geometry is given by the superposition of all the deformations described above. The principle of stress superposition has been long established and applied (e.g. the application of the method developed by Fadum (1941) for defining settlement under the corner of a rectangular foundation). Different idealised geometrical assumptions (see the above descriptions) are taken for the deformations described above, and in reality this will lead to discontinuities in the estimation of the deformation caused by the stress increments. However the representation of the fracture as regular channels (Fig. 1), at the start of every loading step provides shape averaging of the unknown real fracture form. Therefore the deformation error due to the geometrical assumptions of the channel approximations is not cumulative, and it is questionable given the simplistic fracture representation whether a more detailed treatment of the deformation is applicable at this stage.

The volume of the fracture is calculated by considering the deformation of the various geometrical elements, and their effect on the original volume. The deformation is divided into a radial deformation, a box deformation and a fracture wall deformation, Fig. 10a, b.

$$\Delta V_r = \pi\,\Delta r^2 \tag{26}$$

$$\begin{aligned} \Delta V_c = {} & (2r \times (x-2r)) \\ & -((2r-2\rho_b-\rho_c)(x-2r-2\rho_l)) \end{aligned} \tag{27}$$

The total displacement of the fracture wall in terms of a volume (Fig. 11b), assuming unit depth is given by the integral of Eq. (19), along the entire width of the channel. According to Bronstein and Semedjajew (1977) and substituting in the integral, the displacement is given for a unit width by

$$\begin{aligned} \Delta V_w = {} & nc\cdot 8\left(1-\upsilon^2\right)\frac{\Delta\sigma_w}{E} \\ & \times\left[\frac{1}{2}\left(\begin{array}{c} \frac{x}{2} - r\sqrt{\left(\frac{x}{2}\right)^2 - \left(\frac{x}{2}-r\right)^2} \\ +\left(\frac{x}{2}\right)^2 \sin^{-1}\frac{\frac{x}{2}-r}{\frac{x}{2}} \end{array}\right)\right] \end{aligned} \tag{28}$$

DOI 10.1007/s10040-005-0455-4

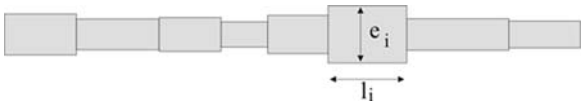

Fig. 11 Approximation of the cross section of a fracture using rectangles, after Baraka-Lokmane et al. (2003)

The change in volume of the fracture is given by

$$\Delta f_v = \Delta V_r + \Delta V_c + \Delta V_w \tag{29}$$

The change in volume of the fluid in the fracture as a result of fluid compression is

$$\Delta f_f = \rho_f f_v \tag{30}$$

As the stress increases so does the number of contacts. The number of contacts is calculated in accordance with Eq. (3). The calculation of the new contact area in the fracture is defined by assigning each contact an equal contact area. The contact area for each contact (Ca) is dependent upon the minimum (min Ca) and maximum (max Ca) contact area allowed and the number of contacts.

$$tCa = \min tCa + \left((nc - \min nc)\left(\frac{\max tCa - \min tCa}{\max nc - \min nc}\right)\right) \tag{31}$$

Fracture parameters

The storage S (m/Pa) of the fracture is given by

$$S = \frac{\Delta f_v + \Delta f_f}{\Delta \sigma f_a} \tag{32}$$

Baraka-Lokmane et al. (2003) give the effective aperture of a fracture system comprising several different discrete elements as

$$e_{nz} = \left[\frac{\sum_{i=1}^{m_{nz}} \left(e_i^3 \cdot l_i\right)}{\sum_{i=1}^{m_{nz}} \left(e_i \cdot l_i\right)}\right]^{\frac{1}{2}} \tag{33}$$

Illustrated in Fig. 11, where m_{nz} is the number of rectangles representing fracture n in the cross section z to be considered.

For a simplified assessment of the hydraulic conductivity of the fracture, by examining equation Eq. (33) it can be seen that using the modelling assumptions here (Fig. 3) the value l_i is constant in contrast to Baraka-Lokmane et al. (2003), therefore the effective fracture aperture of the open fracture (not including the area covered by contact) can be given by Eq. (8). Baraka-Lokmane et al. (2003) then went on to calculate the harmonic average of a series of fracture slices in series along the flow path. In this case the fracture apertures of each section in 3D have the same distribution due to the fractal geometry, and therefore Eq. (8) provides the effective aperture for the determination of the permeability of the sample. Given the fracture aperture, e, equal to $2r$, then the fracture permeability is then given by

$$k_f = \frac{e^2}{12} \tag{34}$$

It follows then that the flow through the fracture for a pressure gradient i *(Pa/m)* is given as

$$Q = \frac{e^2}{12\mu} Ai \tag{35}$$

where A is the open cross sectional area of the fracture through which flow is occurring $(1-tCA)e$ and μ the dynamic viscosity.

In hydrogeology, the equivalent permeability of the system is often considered. Here the formulation for determining the equivalent permeability, i.e. that for a 1-m^2 cross sectional area containing the fracture to provide for the flow in the system, can be derived from Eq. (35) as

$$k_e = \frac{e^3}{12}(1 - tCa) \tag{36}$$

related to the cubic law after Witherspoon et al. (1980).

Roughness in the fracture system is inherently included in the fractal distribution which converts itself into an aperture distribution, but in this form the effect of viscous forces or increased tortuosity as a result of flow channelling are not taken into account. A number of approaches to quantify the effects of roughness on flow through fractures are given by de Marsily (1986). A key paper to understanding channel flow was presented by Tsang and Tsang (1987). Schrauf and Evans (1986) reconstructed the fracture surface as a series of parallel pipes and derived a quadratic relationship of the fracture apertures to the flow within the pipes. Sisavath et al. (2000) assessed in detail the hydraulic radius approximation, the Saint-Venant approach and the Aissen approach for estimating the permeability of a fracture from the asperity distributions and consequent flow channels created. Zimmerman and Bodvarsson (1996) cover in detail the derivation of the hydraulic conductivity from the aperture distribution, based on Navier Stokes equations and the Reynolds Lubrication approximation. They provide an equation, Eq. (37), relating the standard deviation of the aperture with the average aperture size and include a function of the contact area to define the hydraulic aperture. They tested this formulation against a series of results in the literature and found it to give a good approximation of fracture conductivity.

$$e^3 \approx \langle h \rangle^3 \left[1 - 1.5\sigma_h^2 / \langle h \rangle^2\right][1 - 2c] \tag{37}$$

Here $\langle h \rangle$ is the average aperture size, σ_h is the standard deviation of the aperture size, and c is the contact area between the fracture surfaces.

The simplified form of predicating the permeability, Eq. (36), is applied as it seems questionable whether the

 DOI 10.1007/s10040-005-0455-4

increased accuracy gained by applying Eq. (37) will add to the interpretive information gained by applying the closure model presented here given the shape averaging applied to the fracture voids.

Model verification: experimental closure of a single fracture

The purpose of the development of the model described above was eventually to determine the importance of thermo-hydro-mechanical processes at the geothermal reservoir scale e.g. consolidation during hydraulic testing and associated thermo-mechanical effects. In particular, the experimental investigation of the geomechanical characteristics of the KTB borehole, (Emmermann and Lauterjung 1997), were of foremost importance.

The stress profile along the depth of the KTB boreholes has been investigated in detail by Brudy et al. (1997). As confirmed by Baisch et al. (2002) the stress field in the crust is dominated by the presence of fracture zones and the corresponding normal stress across those fractures combined with their resistance to movement. The total normal stress across the fracture coupled with the fracture fluid pressure, the material elastic and plastic properties and corresponding deformation has an effect on the fracture opening and thereby the permeability, porosity and storage of the fracture system. Durham (1997) experimentally investigated the effect of confining pressure on a fracture taken from circa 3,800 m in the KTB pilot hole, measuring the closure of the fracture and the corresponding permeability. These results are taken and fitted with the geomechanical model described here using the known elastic parameters from the KTB site.

Figure 12 presents a fit of the experimental results obtained from Durham's work and those predicted by the model described above. The "fracture permeability," here k_d, given by Durham in his Fig. 2 refers to "the fracture permeabilities for producing the same water flux in the same pressure gradient." distributed through the bulk of the sample. The relationship between the aperture of the fracture and the k_d is given by:-

$$k_d = \frac{2e^3}{12\pi r}\mu \tag{38}$$

Here r is the radius of the sample Durham used to determine the permeability of the fracture.

A comparison of the parameters used to fit the experimental data and parameters available from the literature are given in Table 1.

The value of the elastic modulus for the laboratory investigation is reported by the KTB-workgroup rockmechanics (2005). The values of the poison's ratio comes from geophysical investigation described by Brudy et al. (1997). The geometrical parameters are almost identical to the geometrical parameters indicated by Durham (1997).

The fit of the experimental results can be seen to be extremely good. Based on this fit the model can be applied to

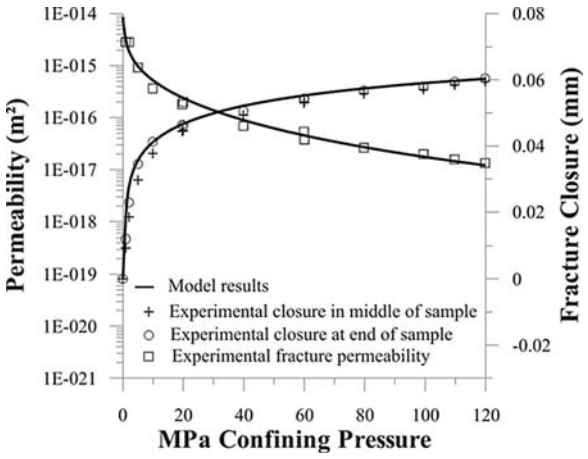

Fig. 12 Comparison of experimental (Durham 1997) and modelled results

describe the geomechanical changes in the hydraulic characteristics of a fracture network under changes in effective stress due to fluid injection and heat extraction. For example as a first approximation of the equivalent permeability and storage of a shear zone with a fracture density f_d of 10 fractures per meter is given in Fig. 13. The equivalent permeability for the shear zone k_s (m^2) is given by the multiplication of the fracture density by the equivalent permeability of a single fracture, Eq. (39), provided by the closure model. The equivalent storage of the shear zone S_s is given by the multiplication of the storage provided by a single fracture S_f (m^3/Pa) from the closure model with the fracture density, added to the bulk volume change of the rock S_b (m^3/Pa) due to the volumetric strain in the rock body Eq. (40) and (41) derived from Davies and Selvadurai (1996). Here the interaction of the fractures with one another is not accounted for, an issue which will be covered in later work.

$$k_s = k_{eq} f_d \tag{39}$$

$$S_s = S_f f_d + S_b \tag{40}$$

$$S_b = \frac{3(1-2\upsilon)}{E} \tag{41}$$

Results such as those illustrated in Fig. 13 may be incorporated into numerical models e.g. the finite element solution procedure, Kolditz (2002), linking effective stress related to pressure and temperature conditions resulting from fluid flow or heat transport to the fracture or shear zone parameters.

Conclusions

A geomechanical model is presented which describes fracture closure under effective stress and the change in parameters such as storage, permeability, porosity and aperture. The model uses geometrical considerations based on a fractal distribution of apertures on the fracture surface, and applies well-established analytical elastic deformation solutions to calculate the strain deformation resulting from

 DOI 10.1007/s10040-005-0455-4

Table 1 Model parameters and literature parameters for the laboratory investigation

Parameter	Model	Literature	Source
Elastic modulus (GPa)	55	55	KTB workgroup Rockmechanics (2005)
Poisson's ratio	0.28	0.28	Brudy et al. (1997)
Init. contact area	15%	10%	Durham (1997)
Min. number of contacts	10	Not avail	
Max. number of contacts	500	Not avail	
Init. equivalent aperture opening (mm)	0.068	0.067	Durham (1997)

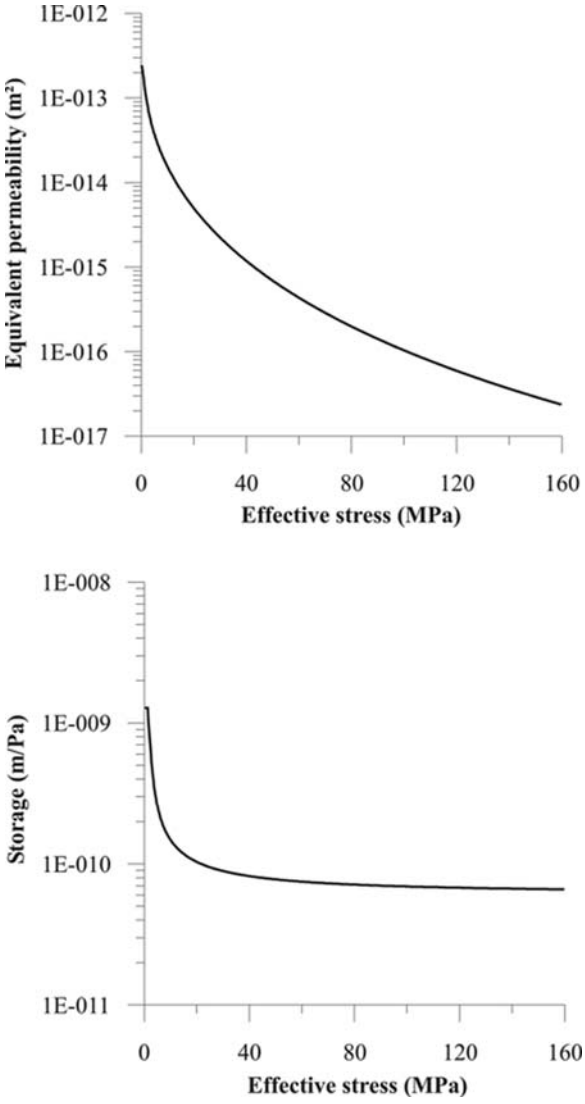

Fig. 13 Predictive modelling of permeability and storage of a shear zone

changes in the normal effective stress. Both the asperity deformation in the fractures and the deformation in the rock body are taken into account.

The fractal approach allows the closure model to predict three-dimensional results for a two dimensional model. In addition the statistical distribution of the contact heights, and thereby the number of contacts between the fracture surfaces under a certain load provides the key to understanding the form of the closure curve, and the parameters coupled to this behaviour.

Consideration of the mathematical formulation of the model indicated that at extreme values of closure, where the fracture is represented as a series of minute channels with circular cross-sections, that stress alone cannot be responsible for total fracture closure. The sealing of fractures to fluid flow must be a consequence of a none-elastic process, such as viscous deformation or pressure solution and deposition.

The model was applied with success at a laboratory scale to measure the closure of a single fracture. At the laboratory, scale experimental data on the closure of a fractured sample from the KTB borehole was modelled accurately. Fitting parameters comprising the elastic constants match independently measured parameters closely. Finally, the model was used to estimate the elastic behaviour of a shear zone comprising several similar fractures to alterations in effective stress.

Acknowledgments The authors wish to thank W. Durham for the provision of the original experimental data and his help in analysis of the data, the Geo-Forschungs Zentrum (GFZ), Potsdam and the various field crews and the staff of the KTB laboratory. We thank the German Science Foundation (Deutsche Forschungsgemeinschaft) for funding (Sa 501/16).

References

Babadagli T, Develi K (2000) Fractal analysis of natural and synthetic fracture surfaces of geothermal reservoir rocks. In: Proceedings of World Geothermal Congress 2000, Kyushu—Tohoku, Japan, May 28–June 10, 2000

Bai T, Pollard DD, Gross MR (2000) Mechanical prediction of fracture aperture in layered rocks. J Geophys Res B: Solid Earth 105(1):707–721

Baisch S, Bohnhoff M, Ceranna L, Tu Y, Harjes HP (2002) Probing the crust to 9-km depth: fluid-injection experiments and induced seismicity at the KTB superdeep drilling hole, Germany. Bull Seismolog Soc Am 92(6):2369–2380

Baraka-Lokmane S, Liedl R, Teutsch G (2003) Comparison of measured and modelled hydraulic conductivities of fractured sandstone cores. Pure Appl Geophys 160:909–927

Baria R, Baumgartner J, Rummel F, Pine RJ, Sato Y (1999) HDR/HWR reservoirs: concepts, understanding and creation. Geothermics 28(4/5):533–552

Barton N, Bandis S (1990) Review of predictive capabilities of jrc-jcs model in engineering practice. In: Proc Int Symp on Rock Joints (Leon, June 4–6, 1990). AA Balkema, pp 603–610

Beeler NM, Hickman SH (2001) A note on contact stress and closure in models of rock joints and faults. Geophys Res Lett 28(4):607–610

Beeler NM, Hickman SH (2004) Stress-induced, time-dependent fracture closure at hydrothermal conditions. J Geophys Res 109(B2):1–16

Belfield WC (1994) Multifractal characteristics of natural fracture apertures. Geophys Res Lett 21(24):2641–2644

 DOI 10.1007/s10040-005-0455-4

Bieniawski ZT (1989) Engineering rock mass classification. Wiley, New York
Bour O, Davy P (1997) Connectivity of random fault networks following a power law fault length distribution. Water Resour Res 33(7):1567–1584
Boussinesq J (1878) Équilibre d'élasticité d'un solide isotrope sans pesanteur, supportant différents poids (elasticity equilibrium of an isotropic solid body supporting different loads, in the absence of gravity). C R Acad Sci Paris 86:1260–1263
Bronstein IN, Semedjajew KA (1977) Taschenbuch der mathematik (handbook of mathematics), Harri Deutsch 3–87144–0167
Brown SR, Scholz CH (1985) Closure of random elastic surfaces in contact. J Geophys Res 90:5531–5545
Brudy M, Zoback MD, Fuchs K, Rummel F, Baumgartner J (1997) "Estimation of the complete stress tensor to 8 km depth in the KTB scientific drill holes: Implications for crustal strength. J Geophys Res 102:18453–18475
Buscheck TA, Rosenberg ND, Gansemer J, Sun Y (2002) Thermohydrologic behavior at an underground nuclear waste repository. Water Resour Res 38(3):101–1019
Davies RO, Selvadurai APS (1996) Elasticity and geomechanics, Cambridge University Press, ISBN: 0-521-49506-7
de Marsily G (1986) Quantitative hydrogeology: Groundwater hydrology for engineers, Academic Press, ISBN: 0-12-208916-2
Durham WB (1997) Laboratory observations of the hydraulic behavior of a permeable fracture from 3,800 m depth in the KTB pilot hole. J Geophys Res 102:18405–18416
Emmermann R, Lauterjung J (1997) The German continental deep drilling program KTB: overview and major results. J Geophys Res 102:18179–18201
Evans M, Hastings N, Peacock B (2000) Statistical distributions. Wiley, New York, 0-471-37124-6
Fadum RE (1941) Influence values for vertical stress in a semi-infinite solide due to surface loads. School of Engineering, Harvard University
Fomin S, Hashida T, Shimizu A, Matsuki K, Sakaguchi K (2003) Fractal concept in numerical simulation of hydraulic fracturing of the hot dry rock geothermal reservoir. Hydrol Process 17(14):2975–2989
Giroud JP (1968) Settlement of a linearly loaded rectangular area. J Soil Mech Found Div, ASCE 94(SM4):813–835
Glover PWJ, Matsuki K, Hikima R, Hayashi K (1998a) Fluid flow in synthetic rough fractures and application to the hachimantai geothermal hot dry rock test site. J Geophys Res 103(B5):9621–9636
Glover PWJ, Matsuki K, Hikima R, Hayashi K (1998b) Synthetic rough fractures in rocks. J Geophys Res 103(B5):9609–9620
Glover PWJ, Matsuki K, Hikima R, Hayashi K (1999) Characterising rock fractures using synthetic fractal analogues. Geotherm Sci Technol 6
Greenwood JA, Williamson J (1966) Contact of normally flat surfaces. In: Proc R Soc Lond, pp 300–319
Hausdorff F (1919) Dimension und äußeres maß. (Dimension and external length). Math Ann 79:157–179
Jaeger JC, Cook NGW (1979) Fundamentals of rock mechanics, 3rd edn. Chapman and Hall, New York, 539 pp
JNC (1999) Japan nuclear cycle development institute: H12 : Project to establish the scientific and technical basis for hlw disposal in Japan, supporting report1 geological environment in Japan. http://www.jnc.go.jp
Johnson K (2001) Contact mechanics. Cambridge University Press, Cambridge452p ISBN: 0-521-34796-3
Kessels W (2000) Elastische eigenschaften von klüften und interpretation hydraulischer tests- untersuchungen im rahmen des KTB—projektes (elastic characteristics of fractures and the interpretation of hydraulic tests and experimental investigation relating to the KTB project). In: 3. Workshop Kluft-Aquifere Gekoppelte Prozesse in Geosystemen, Institut für Strömungsmechanik und Elektron. Rechnen im Bauwesen der Universität Hannover
Kolditz O (2002) Computational methods in environmental fluid mechanics. Springer, Berlin Heidelberg New York, ISBN: 3-540-42895-x
KTB workgroup rockmechanics (2005) http://www.icdp-online.de/sites/ktb/
Laubscher DH (1977) Geomechanics classification of jointed rock masses—mining applications. Trans Inst Min Metall (Sect A: Min Ind) 86:A1–A8
Manzocchi T (2002) The connectivity of two-dimensional networks of spatially correlated fractures. Water Resour Res 38(9):1–1 to 1–20
Matsuki K, Wang EQ, Sakaguchi K, Okumura K (2001) Time-dependent closure of a fracture with rough surfaces under constant normal stress. Int J Rock Mech Min Sci 38(5):607–619
McDermott CI, Randriamanjatosoa AL, Tenzer H, Sauter M, Kolditz O (2005) Pressure dependent hydraulic flow, heat transport and geo-thermo-mechanical deformation in HDR crystalline geothermal systems: preliminary application to identify energy recovery schemes at Urach spa. In: Proceedings World Geothermal Congress 2005, Antalya, Turkey, April 2005
McDermott CI, Sauter M, Liedl R (2003) New experimental techniques for pneumatic tomographical determination of the flow and transport parameters of highly fractured porous rock samples. J Hydrol 278(1–4):51–63
Montemagno CD, Pyrak-Nolte LJ (1995) Porosity of natural fracture networks. Geophys Res Lett 22(11):1397–1400
Myer LR (2000) Fractures as collections of cracks. Int J Rock Mech Min Sci 37:231–243
NAGRA Nationale genossenschaft für die lagerung radioaktiver abfälle (national coorperative for the disposal of radioactive waste)
Nicholl MJ, Rajaram H, Glass RJ, Detwiler R (1999) Saturated flow in a single fracture: evaluation of the reynolds equation in measured aperture fields. Water Resour Res 35(11):3361–3374
Ogilvie SR, Isakov E, Taylor CW, Glover PWJ (2003) Characterization of rough-walled fractures in crystalline rocks. Geol Soc Spec Publ 214:125–141
O'Sullivan MJ, Pruess K, Lippmann MJ (2001) Geothermal reservoir simulation; the state of practice and emerging trends. Geothermics 30(4):395–429
Papanastasiou P (2000) Hydraulic fracture closure in a pressure-sensitive elastoplastic medium. Int J Fract 103(2):149–161
Poulos HG, Davis EH (1974) Elastic solutions for soil and rock mechanics. Wiley, New York
Renner M, Sauter M (1997) Heat as natural tracer: characterization of a conduit network in a karst aquifer using temperature measurements of the spring water. In: Günay G, Johnson AI (eds) Karst waters environmental impacts. Balkema, Rotterdam, pp 423–431
Rutqvist J, Stephanson O (2003) The role of hydromechanical coupling in fractured rock engineering. Hydrogeol J 11:7–40
Schrauf TW, Evans DD (1986) Laboratory studies of gas flow through a single natural fracture. Water Resour Res 22
Sisavath S, Jing XD, Zimmerman RW (2000) Effect of stress on the hydraulic conductivity of rock pores. Phys Chem Earth(A) 25(2):163–168
Smith GN, Smith IGN (1998) Elements of soil mechanics. Blackwell Science Professional, Oxford ISBN: 0-632-04126-9
Tsang YW, Tsang CF (1987) Channel model of flow through fractured media. Water Resour Res 23(3):467–479
Wang JSY, Narasimhan TN, Scholz CH (1988) Aperture correlation of a fractal fracture. J Geophys Res 93(B3):2216–2224
Watanabe K, Takahashi H (1995) Fractal geometry characterization of geothermal reservoir fracture networks. J Geophys Res 100(B1):521–528
Wels C, Smith L, Vandergraaf TT (1996) Influence of specific surface area on transport of sorbing solutes in fractures: an experimental analysis. Water Resour Res 32(7):1943–1954
Witherspoon PA, Wang JSY, Iwai K, Gale JE (1980) Validity of cubic law for fluid flow in deformable rock fracture. Water Resour Res 16(6):1016–1024

 DOI 10.1007/s10040-005-0455-4

Xie H, Wang JA, Kwasniewski MA (1999) Multifractal characterization of rock fracture surfaces. Int J Rock Mech Min Sci 36(1):19–27

Zhou HW, Xie H (2003) Direct estimation of the fractal dimensions of a fracture surface of rock. Surf Rev Lett 10(5):751–762

Zimmerman RW (1991) Compressibility of sandstones, developments in petroleum science, 29, Elsevier ISBN 0-444-88325-8

Zimmerman RW, Bodvarsson GS (1996) Hydraulic conductivity of rock fractures. TranspPor Med 23:1–30

Zimmerman RW, Myer LR, Cook NGW (1994) Grain and void compression in fractured and porous rocks. Int J Rock Mech Min Sci 31(2):179–184

Zimmermann G, Korner A, Burkhardt H (2000) Hydraulic pathways in the crystalline rock of the ktb. Geophys J Int 142(1):4–14

Zimmermann G, Burkhardt H, Engelhard L (2003) Scale dependence of hydraulic and structural parameters in the crystalline rock of the KTB. Pure Appl Geophys 160(5–6):1067–1085

 DOI 10.1007/s10040-005-0455-4